WELDING RESEARCH

SUPPLEMENT TO THE *WELDING JOURNAL*, JULY 1993
Sponsored by the American Welding Society and the Welding Research Council

Metal Transfer in Pulsed Current Gas Metal Arc Welding

A static force balance analysis was used to estimate the melting rates of the electrodes during pulsed gas metal arc welding

BY Y.-S. KIM AND T. W. EAGAR

ABSTRACT. In order to achieve one drop per pulse operational conditions with pulsed current GMAW, it is necessary to control both the drop size at the peak current and the melting rate of the electrode. In this study, a static force balance analysis was used to predict the droplet size at the peak current and a weighted sum of the melting rates measured under Direct Current Electrode Positive (DCEP) welding was employed to estimate the melting rate with pulsed current. Combining the static force balance analysis and the weighted sum method, a model is proposed to predict the optimal conditions of one drop per pulse operation. The model is found to be in good agreement with the experimental results when the base current and the load duty cycle are small. When the base current increases above 220 A and the load duty cycle exceeds 10% using 1.6-mm-diameter steel electrodes, the prediction of the model deviates significantly from the experimental results. The discrepancy between the model and the experimental results is discussed and is shown to be due to tapering of the electrode tip at high welding currents.

Y. S. KIM is Assistant Professor, Department of Metallurgy and Materials Science, Hong Ik University, Seoul, Korea, and T. W. EAGAR is Co-Director, Leaders for Manufacturing Program, Richard P. Simmons Professor of Metallurgy, Department of Materials Science and Engineering, Massachusetts Institute of Technology, Cambridge, Mass.

Introduction

Since the introduction of pulsed current Gas Metal Arc Welding (GMAW-P) in 1962 (Ref. 1), this method of welding has been used widely both in mechanized welding and in robotic welding. With pulsed GMAW, a stable spray metal transfer mode can be obtained at low average currents that would otherwise produce globular transfer with large sporadic drops. Pulsing leads to stable spray metal transfer and formation of a uniform bead shape with shallow penetration. Recent improvements in power supply designs using transistor or frequency converter controls also provide better controllability of the process (Ref. 2).

KEY WORDS

Pulsed Current GMAW
Modeling
Metal Transfer
Electrode Melt Rate
Static Force Balance
Weighted Sum Method
Droplet Size
Optimum Pulsing Freq.
Electrode Tapering
Melting Rates

Pulsing the current introduces additional operational parameters, which include peak current, base current, peak pulse time, and base pulse time, in addition to the variables of DC welding, which include electrode extension, welding current and welding voltage. These extra variables cause difficulty in selecting optimum operating conditions for pulsed current welding. A trial-and-error method is often used to determine these conditions. However, the basic physics of metal transfer in pulsed current welding needs to be understood in order to more successfully control the process.

There have been several attempts to analyze pulsed current welding theoretically (Refs. 3–5). Samati (Ref. 5) predicted the theoretical pulsing frequency by dividing the electrode melting rate by the mass of the drop, and showed good agreement between these predictions and experimental results. However, this agreement is anticipated since there is a range of working solutions instead of a single-valued pulsing condition as shown experimentally by Allum (Ref. 3).

In this study, a theoretical framework is described for prediction of the range of optimum pulsing frequencies. The method uses a combination of the

RESEARCH/DEVELOPMENT/RESEARCH/DEVELOPMENT/RESEARCH/DEVELOPMENT

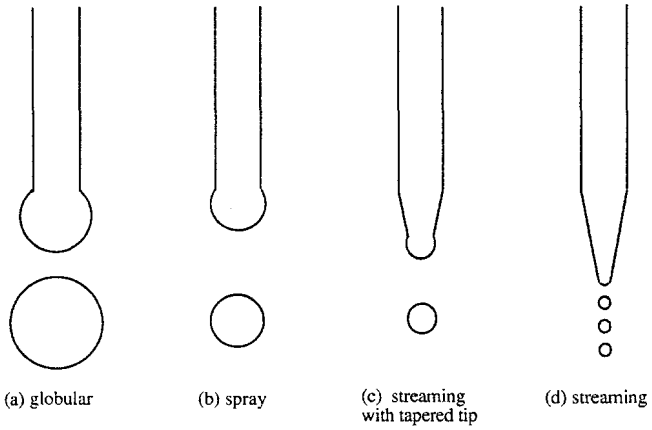


Fig. 1 — Schematic representations of metal transfer modes as welding current increases from A to D.

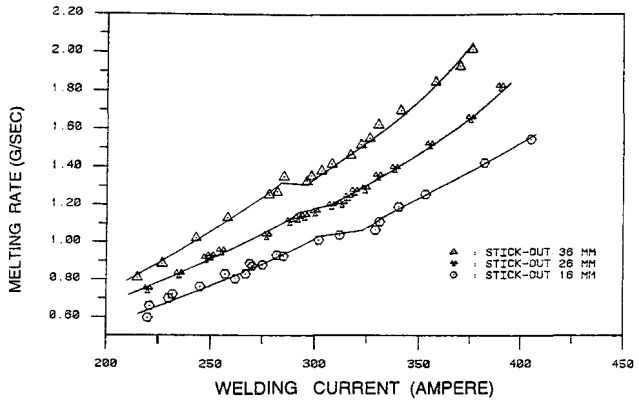


Fig. 2 — Melting rates of steel electrodes (1.6 mm diameter) shielded with Ar-2%O_2.

droplet size predicted from the static force balance theory, and the melting rate from the weighted sum of melting rates at the peak and base currents equivalent to DC welding. This theoretical model is then compared with the experimental results obtained using steel, Ti-6Al-4V and aluminum electrodes.

Theoretical Framework for Pulsed Current GMAW

As one increases the current during DC welding in argon-rich atmospheres, the metal transfer mode changes from globular to spray. With further current increases in the spray current regime, the anode spot increases in size until it begins to climb the sides of the solid cylindrical electrodes. The condensation heat produced by the current on these vertical surfaces causes melting of the cylinder edges (Ref. 11). At sufficiently high currents, this produces a tapered solid electrode tip as seen in Fig. 1. In order to obtain one liquid metal drop with a size similar to the electrode diameter at every pulse, the operating conditions must be such that significant tapering does not occur at the tip of the electrode. If tapering occurs, the pulsed current process degenerates into streaming metal transfer mode (Ref. 7) and it becomes difficult to obtain one drop with each pulse.

Among the four pulsing parameters, which include peak current, peak time, base current and base time, the pulsing frequency and the load duty cycle were used as the operational parameters of interest instead of the more commonly used peak time and base time. Pulsing frequency is defined as 1/(peak time + base time) and load duty cycle as (peak time) / (peak time + base time) X 100 (%). The employment of pulsing frequency and load duty cycle as the operational parameters eliminates some of the complexity of adjusting the process. For instance, if the load duty cycle is kept constant, the pulsing frequency can be changed without affecting the average welding current, which may lead to a relatively constant electrode melting rate. In this manner, it is possible to determine a range of optimum pulsing frequencies at a constant electrode melting rate.

In pulsed current GMAW, a theoretical pulsing frequency is obtained by dividing the electrode melting rate with current pulsing by the mass of one drop :

$$\text{theoretical pulsing frequency} = \frac{\dot{m}_{pulse}}{V_{drop}(I_p)\rho_d} \qquad (1)$$

where:

$\dot{m}_{pulse}$ is the electrode melting rate with current pulsing, $V_{drop}(I_p)$ is the predicted volume of the drop at the peak current, and ρ_d is the density of the drop.

The average melting rate for a square wave current may be estimated as the weighted sum of the DC melting rate at the peak current and at the base current.

$$\dot{m}_{pulse} = \beta \dot{m}(I_p) + (1-\beta)\dot{m}(I_B) \qquad (2)$$

β: load duty cycle

$\dot{m}(I_p)$: DC melting rate at peak current

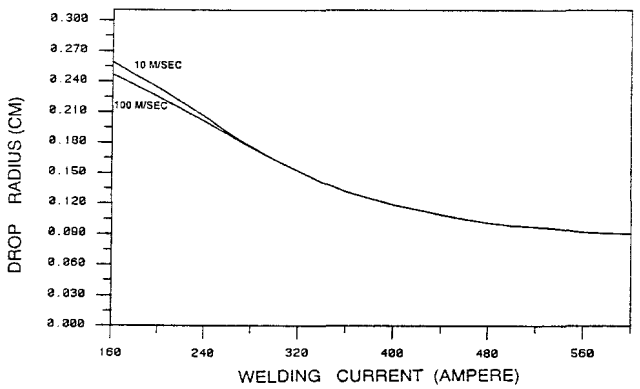


Fig. 3 — The equilibrium droplet size from a 1.6-mm-diameter steel electrode calculated from the static balance theory at two different argon gas speeds (10 m/s and 100 m/s) around drops.

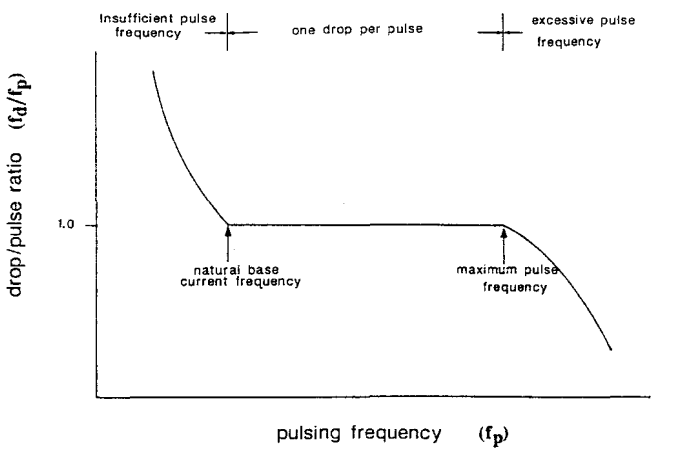


Fig. 4 — Schematic diagram of weld current pulsing.

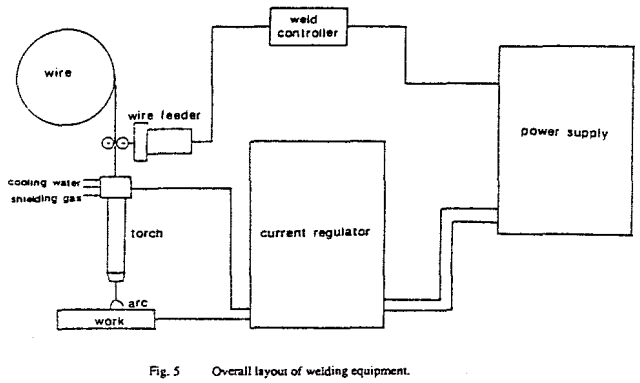


Fig. 5 Overall layout of welding equipment.

Fig. 5 — Overall layout of welding equipment.

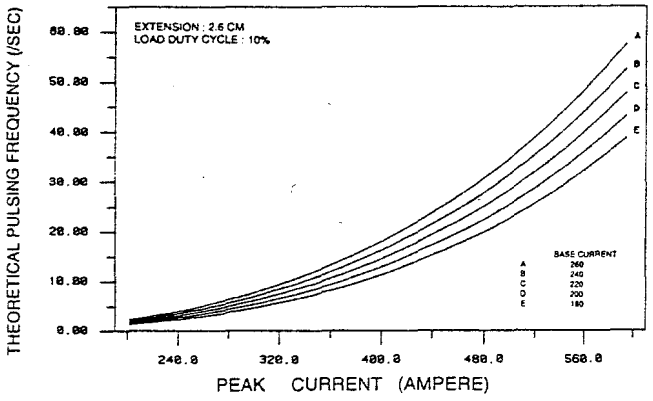


Fig. 6 — Theoretical pulsing frequency for steel electrodes shielded with Ar-2%O_2 as a function of peak current.

$m(I_b)$: DC melting rate at base current

As shown in our previous work (Ref. 8), the melting rate undergoes a transition as the welding current increases as shown in Fig. 2. This transition is related to formation of the taper. Since fully developed tapers have less tendency to form in pulsed current welding, the DC melting rate measured in the pretransition region has been extrapolated to the peak current levels in order to estimate the melting rate at the peak current.

The droplet size in pulsed current welding may be determined at the peak current using the static force balance model. Figure 3 shows the results of this calculation. The higher the peak current, the smaller will be the droplet size. The details of this calculation can be found elsewhere (Ref. 7).

When the pulsing frequency is increased above the theoretical pulsing frequency of Equation 1 with other operational parameters held constant, not every pulse can detach one drop. In other words, the droplet size and the melting rate remain the same; theoretically it is impossible to produce more drops than predicted by the theoretical frequency given by Equation 1. Therefore, the theoretical pulsing frequency is the theoretical maximum pulsing frequency (TMPF) that should be applied to the system. On the other hand, as the pulsing frequency is decreased below the TMPF, each pulse can still produce one drop over a limited range of lower frequencies, but the droplet size becomes larger than the equilibrium droplet size at the TMPF. If the pulsing frequency is decreased further, droplet transfer frequency at the DC base current will eventually become faster than the applied pulsing frequency. Hence the droplet transfer frequency at the DC base current sets the lower limit of the one drop per pulse region. When the pulsing frequency is lower than the limit, the drop will be detached in two modes: one controlled by the base current and the other controlled by the peak current. Therefore, within one cycle of pulsing, several drops may be detached and the size of the droplets will become nonuniform.

Figure 4 schematically shows the concepts of the preceding paragraph. The droplet transfer frequency to pulse frequency ratio on the vertical axis is defined as the actual droplet transfer rate divided by the applied pulsing frequency. When the droplet to pulse frequency ratio is equal to one, each pulse produces one drop. This is the optimum pulsing frequency region for practical welding. When the droplet to pulse frequency ratio is larger than 1.0, the natural frequency becomes larger than the pulsing frequency, hence insufficient pulse frequency is present. Finally, when the droplet to pulse frequency ratio is less than 1.0, pulsing becomes so fast that not every pulse can produce a drop, hence the pulse frequency is excessive.

Experimental Procedures

Mild steel (AWS E70s-3), aluminum alloy (AA1100, AA5356), and titanium alloy (Ti-6Al-4V) were used in the experimental portion of this study. The shielding gases were pure argon and argon-2% oxygen. The welding equipment included a constant current-type power supply, a transistorized current regulator, and a voltage-controlled electrode feed with a low inertia motor. The power supply could provide a total out-

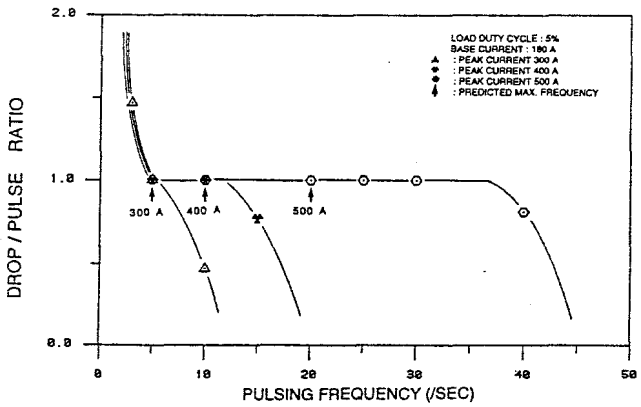


Fig. 7 — Optimum pulsing frequency regions for steel electrodes shielded with Ar-2%O_2. The base current was 180 A and the load duty cycle was 5%.

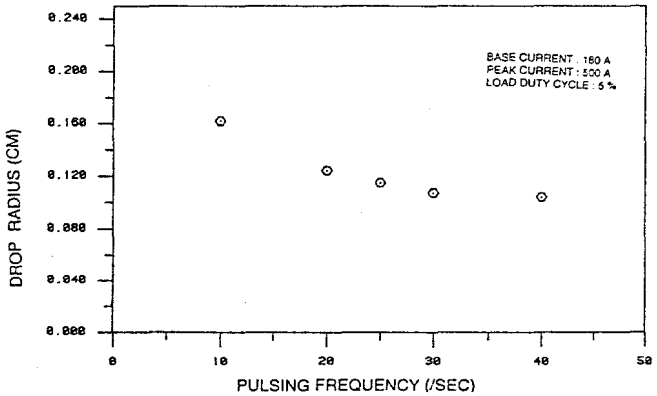


Fig. 8 — Droplet size variation in the range of optimum pulse frequency for steel electrodes with Ar-2%O_2 shielding. The peak current is 500 A.

Table 1 — Conditions used for Pulsed Current Welding

	Peak current (A)	Base current (A)	Frequency (Hz)	Duty cycle %
Mild steel	300, 400, 500	180, 200, 220, 260	5 to 300	5, 10, 20
Aluminum (1100)	300, 400, 500	170, 200	3 to 150	10
Ti-6Al-4V	300, 400, 500	130, 200	3 to 100	10

put power of over 1200 A.

The transistorized current regulator used in this study can supply DC current with less than 1% ripple (Ref. 9). This system uses transistors to control the welding current and is capable of pulsing the DC current to a maximum of 5 kHz for small superimposed signals. The equipment can control pulsing parameters, peak current, base current, peak time and base time, independently from a function generator included with the controller. An alumina tube was inserted into the contact tip of a commercial welding gun leaving only 5 mm for contact length rather than the normal contact length of 24 mm. A transversing weld table was used so that the weld gun could remain at a fixed position. Figure 5 shows the overall layout of the welding equipment.

Analysis of metal transfer was performed using high-speed videography with a backlighted shadow graphic method (Ref. 10). This method excludes most of the intense arc light and transmits most of the laser light by a spatial filter that is placed at the focal point of the objective lens. The high-speed video camera is capable of producing images at a maximum 1000 full frame pictures per second (pps). The droplet transfer rate was measured for 10 s and an averaged droplet transfer rate for each welding condition was calculated. The droplet size was measured from the still image on the screen once every second for 10 s and averaged. The variation in droplet size and frequency is estimated to be ± 5% in most cases.

Melting rates of the electrode were measured using a tachometer that was in contact with the moving wire electrode. The output voltage of the tachometer and of the current shunt, which was filtered by a low band pass filter, was recorded with a high-speed recorder.

The ranges of operational variables for pulsed current welding used in this study are shown in Table1. Based on the initial pulsing frequency, which was determined using predictions from the theoretical model developed in this study, the pulsing frequencies were changed in order to determine the range of pulsing frequencies of one drop per pulse. This range of the pulsing frequencies was judged primarily from the recordings of arc voltage and pulse current on a high-speed recorder and was later analyzed more accurately using high-speed videography. With the high-speed videography, the droplet transfer frequency and the droplet size were determined.

Pulsed Current GMAW with Steel Electrodes

Effect of Peak Current

Figure 6 shows the TMPF calculated from Equation 6 as a function of peak current at various levels of base current. The TMPF increases as the peak current increases because the melting rate of the electrode increases due to the increase in average current and the decrease in droplet size. Using this TMPF as a reference frequency, a series of pulsing frequencies was tested experimentally in order to determine the range of one drop per pulse with other pulsing conditions remaining constant.

Figure 7 shows the regions of pulsing frequency with a 180-A base current at three different peak currents: 300, 400 and 500 A. The load duty cycle used was 5%. As seen in the figure, as the peak current increases, the width of the one-pulse-one-drop (OPOD) region increases. When the peak current is 300 A, the OPOD region is very narrow (4 to 6 Hz). When the peak current increases to 400 A, the range widens to 4 to 12 Hz and, finally, when the peak current is 500 A, the range expands to 4 to 38 Hz. This expansion of the OPOD region as the peak current increases was also observed at different base currents. This expansion of the OPOD region, especially the increase of TMPF with peak current, is due to the increase in the electrode melting rate and the decrease in the droplet size as the peak current increases. The lower bound pulsing frequency, 4 Hz, was not affected by the peak current. This value agrees well with the measured natural DC droplet transfer frequency of 3.5 Hz at a current of

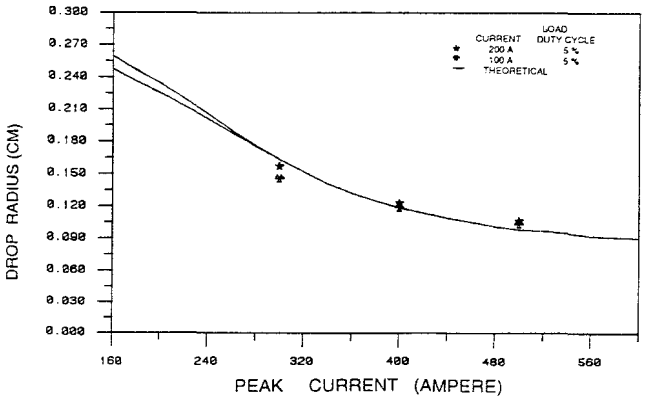


Fig. 9 — Comparison between droplet size from the static force balance theory and minimum droplet size in pulsed current welding for steel electrodes with Ar-2%O_2 shielding.

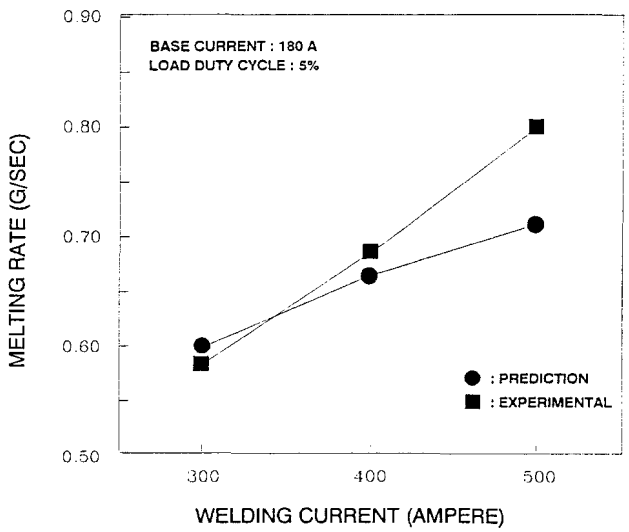


Fig. 10 — Melting rate of steel electrodes at three different peak currents with Ar-2%O_2 shielding.

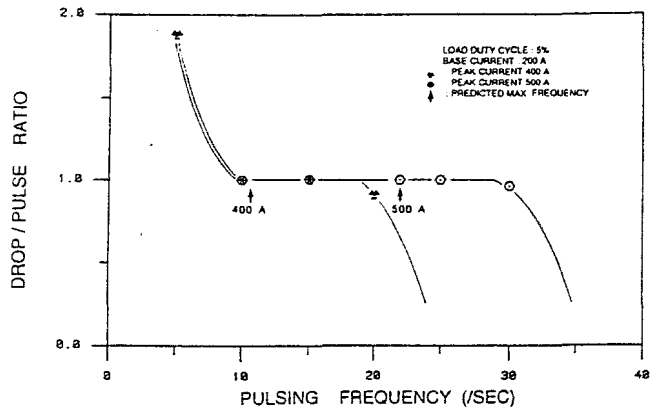


Fig. 11 — Pulsing frequency regions of steel electrodes at a base current of 200 A with Ar-2%O_2 shielding.

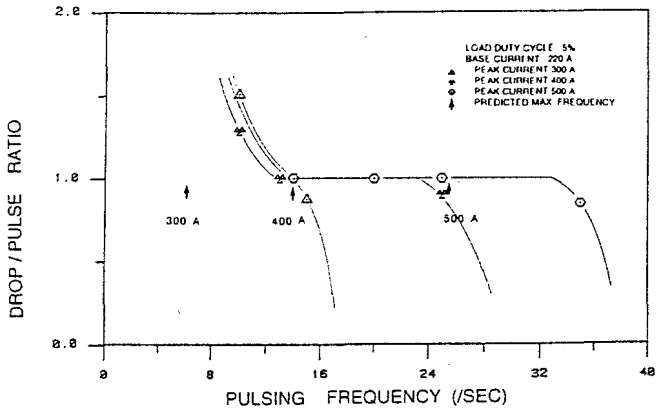


Fig. 12 — Pulsing frequency regions of steel electrodes at a base current of 220 A Ar-2%O_2 shielding.

180 A. However,the TMPF, which are indicated by the arrows in the figure, do not coincide with the measured maximum pulsing frequency.

Figure 8 shows the variation of the droplet size as the pulsing frequency changes at a peak current of 500 A. As the pulsing frequency increases, the droplet size decreases until it reaches a minimum value. This corresponds to the equilibrium droplet size at which the detaching forces at the peak current are just equal to the retaining surface tension force. Figure 9 compares the equilibrium droplet size from the static force balance theory with the experimentally measured minimum droplet sizes at different peak currents. The prediction and the experimental results agree with errors of less than ± 10%. These results show that the static force balance theory can be used to predict the droplet size at various peak currents.

The discrepancy of the TMPF from the experimental results may be caused by two possibilities as one can see from Equation 1: either the equilibrium droplet size is in error or the melting rate predicted from the weighted sum method is in error, or both. Since the predicted equilibrium droplet size agrees reasonably well with the experimentally measured minimum droplet size, the actual melting rate during pulsed current welding was measured to compare with the melting rate predicted from the weighted sum method.

The melting rates measured at different peak currents along with the melting rates predicted from the weighted sum method of Equation 1 are shown in Fig. 10. As mentioned in the previous section, the melting rate for the peak current is calculated from the curve extrapolated from the pretransition melting rate curve of the DCEP welding process. As seen in the figure, the measured electrode melting rate is higher than the calculated melting rate predicted by Equation 1. When the increased melting rate under current pulsing is used in Equation 1, the TMPF at 180 A base current, 500 A peak current, and 5% load duty cycle is calculated to be 30 Hz, which is closer to the experimentally observed 37 Hz. Therefore, this increased melting rate under pulsed current welding must cause a significant portion of the discrepancy between the TMPF and the measured maximum pulse frequency.

Effect of Base Current

Figures 11, 12 and 13 show the experimental results of the droplet to pulse frequency ratio as a function of the pulsing frequency at base currents of 200, 220 and 260 A, respectively. When the base current is 200 (Fig. 11) and 180 A (Fig. 7), the predicted TMPF lie within the OPOD region. As the base current is increased to 220 A as in Fig. 12, the TMPF starts to shift outside of the OPOD region. With peak currents of 400 and 500 A, the TMPF are within the region of OPOD, but with a peak current of 300 A the TMPF becomes smaller than the lower frequency of the OPOD region. When the base current is increased to 260 A, the TMPF of all peak currents becomes smaller than the measured lower limit frequency of the OPOD region.

These large deviations of theoretical prediction from the experimental measurements can be explained from the results of the droplet size measurements in our previous studies (Ref. 7). Around 210 A in DCEP welding the measured droplet size becomes significantly smaller than the droplet size predicted by the static force balance theory due to

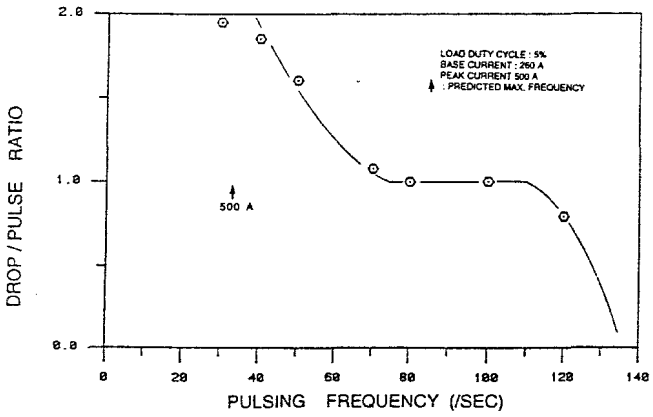


Fig. 13 — Pulsing frequency regions of steel electrodes at a base current of 260 A Ar-2%O_2 shielding.

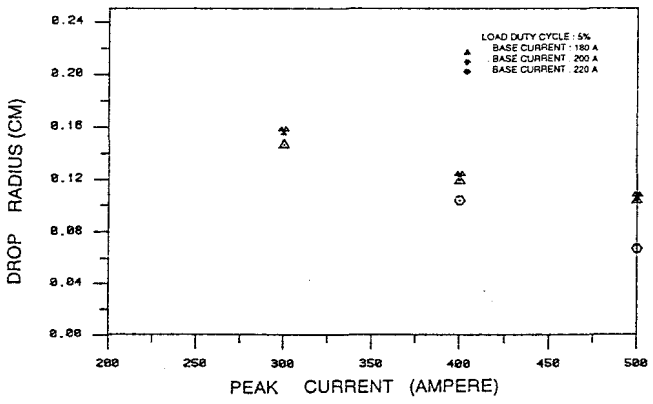


Fig. 14 — The minimum droplet size of steel electrodes at three different base currents Ar-2%O_2 shielding.



Fig. 15 — Partial tapering at the tip of the steel electrode when shielded with Ar-2%O_2. The base current is 220 A and the peak current is 400 A.

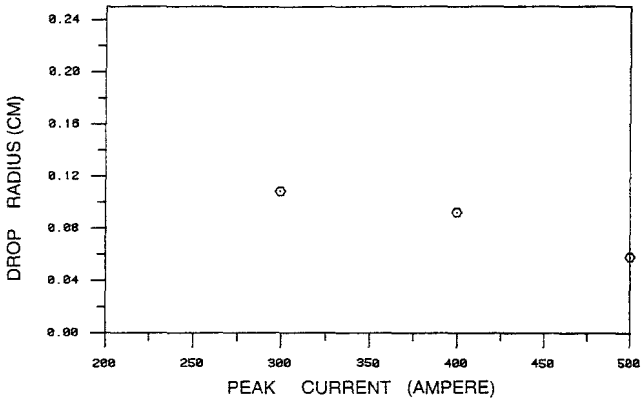


Fig. 16 — The minimum droplet size of steel electrodes at three different peak currents when shielded with Ar-2%O_2. The base current is 180 A and the load duty cycle is 10%.

tapering of the electrode. Therefore, with pulsed welding conditions in which tapering of the electrode occurs, the TMPF, which are calculated by the droplet size predicted from the static force balance theory, will be smaller than the measured droplet transfer frequency. Figure 14 shows the droplet size measured at different base currents when tapering occurs as in Fig. 15. It can be seen that the minimum droplet size is smaller than that predicted by the DC (nontaper) prediction at the 220 base current. Thus, it is believed that it is the formation of a taper that causes the predicted TMPF to be smaller than that measured experimentally. The tendency for tapering of the electrode increases as both base currents and peak currents increase.

Effect of Load Duty Cycle

When load duty cycle is increased to 10%, tapering of the electrode occurs even at low base currents. For instance, with 10% load duty cycle, tapering is observed at a base current of 180 A and a peak current of 400 A. With such a high load duty cycle, the electrode tapers during the peak current period and does not return to a cylindrical shape immediately after the current is lowered to the base current. This phenomenon is especially easy to observe at pulsing frequencies near the lower boundary of the optimum pulsing frequency region.

Since a small amount of tapering can expand the OPOD region by creating decreased minimum droplet sizes, the tapering of the electrode can be beneficial if the degree of tapering is small enough such that droplet sizes similar to the electrode size can be obtained. Figure 16 shows the measured decrease in droplet size due to the partially developed taper seen in Fig. 15. When there is partial tapering of the electrode, the OPOD region is increased significantly as shown in Fig. 17. The pulse frequency working range at a base current of 180 A and a peak current of 400 A with 10% load duty cycle is approximately twice as wide as that with 5% load duty cycle, which produces no partial tapering.

As the load duty cycle is further increased up to 20%, the OPOD region increases significantly because the droplet sizes are further reduced by the well-developed taper on the electrode.

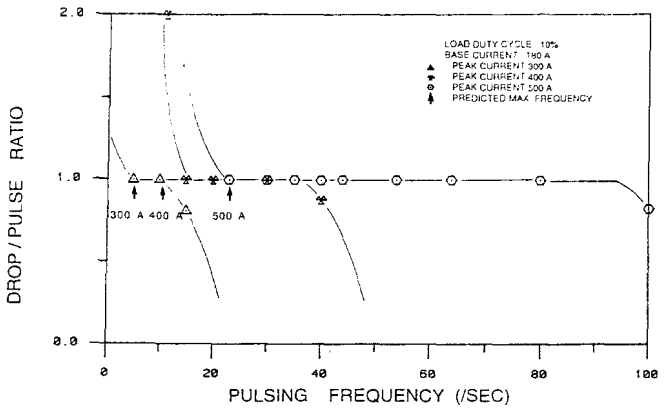


Fig. 17 — The pulsing frequency region of steel electrodes shielded with Ar-2%O_2 at three different peak currents. The width of the optimum pulsing frequency region has increased significantly at 10% load duty cycle.

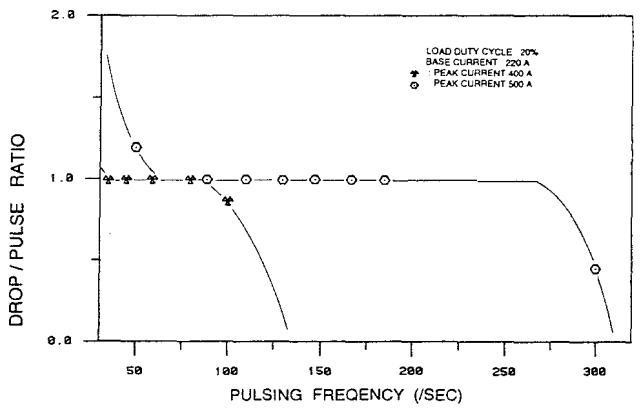


Fig. 18 — The pulsing frequency region of steel electrodes at 20% load duty cycle Ar-2%O_2 shielding. The base current is 220 A.



Fig. 19 — A fully developed taper at peak current during pulsed GMAW. The steel electrode is shielded with Ar-2%O_2.

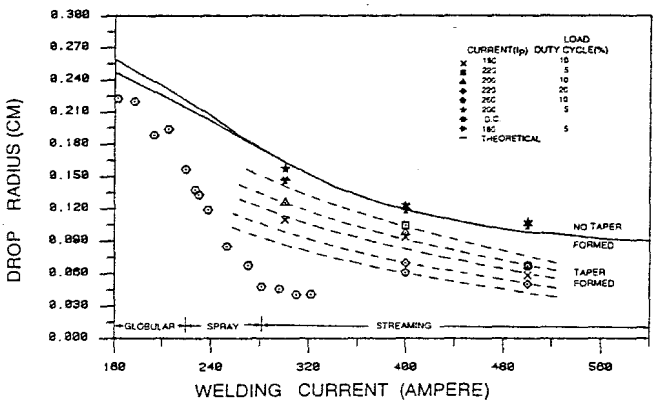


Fig. 20 — The minimum droplet size of steel electrodes shielded with Ar-2%O_2 under different pulsing conditions. Depending on the degree of tapering, the droplet size forms over a range of droplet size.

Figure 18 shows the OPOD range with base current of 220 A and 20% load duty cycle. The minimum droplet sizes measured with pulsed current welding are as small as the droplet sizes obtained with streaming transfer in DC welding. Therefore, it is only possible to achieve one pulse per drop at very high pulsing frequencies under these high duty cycle conditions. In this case, there is no advantage of using pulsed current welding since the droplet size is no longer similar to the droplet size of projected spray transfer; one could use DC streaming transfer just as well.

In pulsed current welding, it is observed that there are various taper shapes depending on the pulsing parameters. For example, there is a fully developed taper as seen in Fig. 19 and a partially developed taper as seen in Fig. 15. As the base current and load duty cycle increase, the tapering becomes larger and will decrease the equilibrium droplet size. Figure 20 shows the minimum droplet sizes measured under different pulse conditions. As seen in this figure, when there is no taper, the droplet size is very close to the theoretical value predicted by the static force balance theory. When the taper starts to develop with increases in the base current and/or the load duty cycle, the droplet size begins to decrease depending on the degree of tapering. Finally, when the pulsing condition develops a fully developed taper (such as with the 20% load duty cycle and 220-A base current), the droplet size approaches the droplet size of streaming transfer in DCEP welding.

The formation of a taper causes various problems in analyzing pulsed current welding; however, tapering provides one important advantage of providing a wider range of the optimum pulsing frequency region. Therefore, by controlling the development of the taper, the OPOD range can be widened, which leads to easier control of the process. The addition of helium to argon shielding gas has been known to suppress the tendency to form a taper (Ref. 11). Thus, the use of helium gas mixtures is expected to widen the range of frequency over which OPOD can be obtained.

Effect of Materials

Ti-6Al-4V and Aluminum 1100 electrodes were also tested. With Ti-6Al-4V electrodes, the general trend of the OPOD region is the same as with the steel electrode. As shown in Fig. 21, the optimum frequency region increases with the peak current. Also, the minimum droplet size decreases with the peak current but is larger than the droplet size predicted from the static force balance theory, which may reflect the repulsive forces experienced in this process.

With Ti-6Al-4V electrodes, tapering was not observed up to 240 A with DCEP welding. However, Fig. 22 shows that a taper forms during pulsed current welding at 200-A base current, 500-A peak current, with 10% load duty cycle, and 20-Hz pulsing frequency. This shows that tapering of the electrode may occur with argon shielding in materials other than steel, but the onset current of tapering is dependent on the properties of the material.

With the aluminum electrode, the OPOD range was measured for 300-, 400- and 500-A peak currents using a load duty cycle of 10%. With these conditions, it was not possible to find any satisfactory optimum pulsing frequency region. With most of the conditions, tapering occurs, leading to streaming transfer. When tapering does not occur, secondary small drops occur after primary droplet detachment as shown in

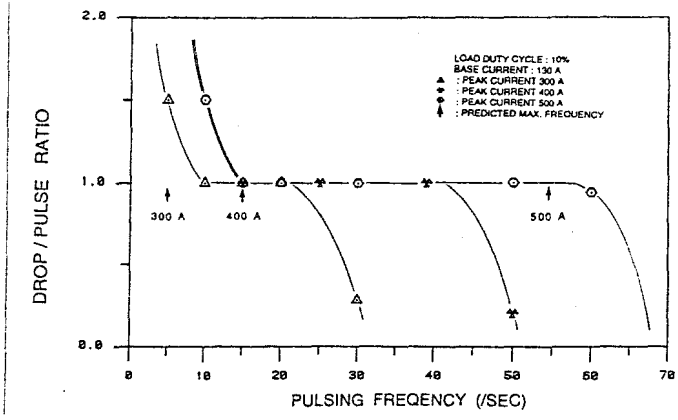


Fig. 21 — The pulsing frequency region with Ti-6Al-4V electrodes shielded with pure argon.

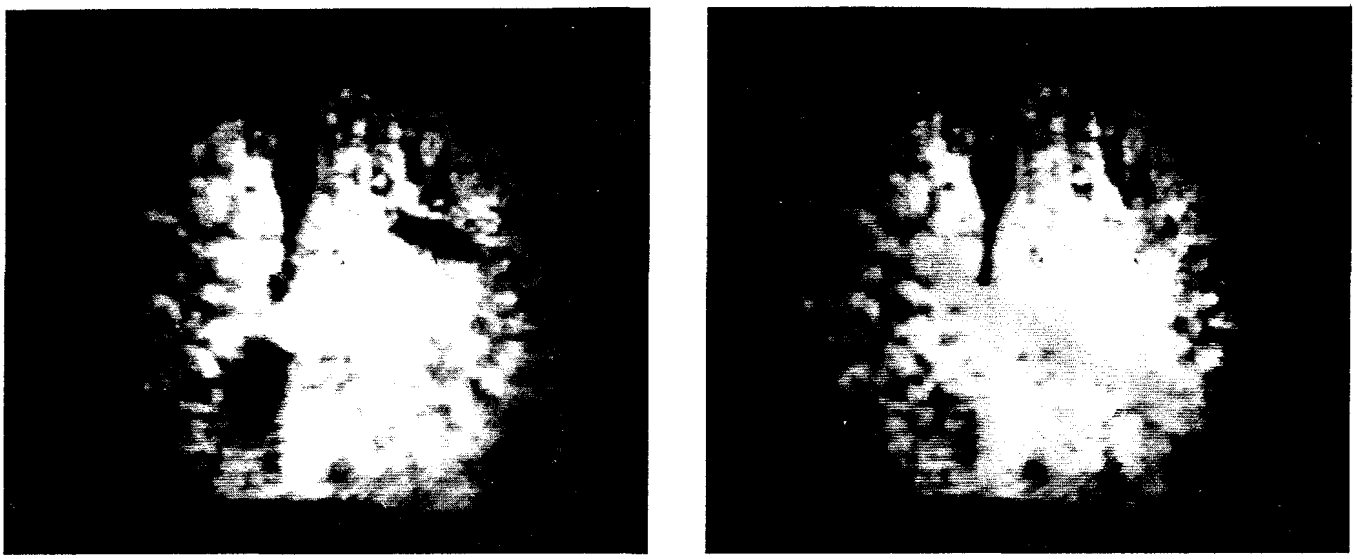


Fig. 22 — Tapering of Ti-6Al-4V electrode with argon shielding. A — Beginning of the tapering; B — an established taper of the electrode. The base current is 200 A and the peak current is 500 A. The load duty cycle is 10%.

Fig. 23. This may be due to the fact that the peak currents used in this study were too high for aluminum. The low surface tension of aluminum causes the detaching force to create too much disturbance in the liquid drop. With lower peak currents and with a lower load duty cycle, there may be a range of optimum pulsing frequencies for aluminum welding.

Further Observations with Pulsed Current GMAW

From the observations made in this study, several important aspects of the pulsed current welding process can be identified. Firstly, peak current has the most significant effect on the OPOD range, as seen in Fig. 7. In general, the higher the peak current, the wider the OPOD range. However, when peak current is increased too much, tapering of the electrode will occur, leading to a streaming transfer mode in which the droplet size is too small to control. Tapering may be suppressed by using a shielding gas consisting of Ar-He mixtures.

Secondly, when welding with steel electrodes using carbon dioxide as a shielding gas, the application of pulsed GMAW will not provide any advantages in controlling droplet size. Since the droplet size remains nearly the same and the mode of metal transfer is repelled transfer (Ref. 11), pulsing of current will not produce projected spray transfer when welding steel electrodes shielded with carbon dioxide.

Thirdly, when welding with steel electrodes using helium as the shielding gas, pulsed current GMAW may produce projected metal transfer in the normal DC range of repelled globular transfer. The repelled metal transfer mode at low welding current transforms into the projected spray transfer mode as welding current increases. Therefore, if the peak current used is greater than the transition current of repelled-projected transition, pulsed current GMAW will produce a projected transfer mode. The same reasoning can be applied when welding with titanium electrodes shielded with argon, which exhibit the same transition phenomenon as the welding current increases.



Fig. 23 — Secondary metal transfer with aluminum electrodes in pulsed current welding. The shielding gas is pure argon.

Conclusions

A theoretical model of pulsed current welding is developed to predict ranges of one pulse per one drop pulse frequency. Experimental results confirm this approach.

The width of the optimum pulsing frequency region increases as the peak current increases. This is due to the fact that the range of droplet sizes available and the melting rate increase as the peak current increases.

The static force balance theory can predict the droplet size at a given peak current provided that there is no significant tapering at the tip of the electrode.

The melting rates under pulsing current conditions are greater than melting rates calculated using a weighted sum of the melting rate (for DC currents) at the peak current and at the base current. The workable ranges of base current and load duty cycle can be expanded when tapering of the electrode can be suppressed. This may be achieved by adding helium and/or carbon dioxide to the argon gas.

Acknowledgments

This research was funded by a grant from the United States Department of Energy under contract number DE-FG02-85ER-13331.

References

1. Needham, J. C. 1962. Control of transfer in aluminum consumable electrode welding. *Physics of Welding Arc,* The Institute of Welding, London, pp. 114-124.

2. Shimada,W., and Ukai, J. Effects of pulsed current control on welding quality improvement. IIW Document # XII-B-11-81.

3. Quintino, L., and Allum, C. J. 1984. Pulsed GMAW: interaction between process parameters — part II. *Welding and Metal Fabrication,* Vol. 4, pp. 126-129.

4. Quintino, L., and Allum, C. J. 1984. Pulsed GMAW: interaction between process parameters — part I. *Welding and Metal Fabrication,* Vol. 3, pp. 85-89.

5. Samati, Z. 1986. Automatic pulsed MIG welding. *Metal Construction,* Vol. 18, No.1, pp. 33R-44R.

6. Lesnewich, A. 1958. Control of melting rate and metal transfer in gas-shielded metal-arc welding, Part I — Control of electrode melting rate. *Welding Journal* 37(8):343-s to 353-s.

7. Kim, Y. S., and Eagar, T. W. Analysis of metal transfer in gas metal arc welding. *Welding Journal* 71(6):269-s to 278s..

8. Kim, Y. S., and Eagar, T.W. 1989. Temperature distribution and energy balance in the electrode during GMAW. Proc. of Trends in Welding Research, Gatlinburg, TN.

9. Eickhoff, S. T. 1988. Gas-metal arc welding in pure argon. M.S. thesis, MIT, Cambridge, Mass.

10. Allemand, C.D., Schoeder, R., Ries, D.E., and Eagar, T.W. 1985. A method of filming metal transfer in the welding arc. *Welding Journal* 64(1):45–47.

11. Kim, Y. S. 1989. Metal transfer in gas metal arc welding. Ph.D. thesis, MIT, Cambridge, Mass.

Plan now to attend!

Commercialization of Advanced Joining Technology Through Industry-Government Partnering

September 27-28, 1993 - Boulder, Colorado

This conference, sponsored by the American Welding Society, will describe the mechanisms (CRADA, licensing, etc.) by which the government can work with industry; make the welding industry aware of government sponsored research that is available for commercialization; offer the concept of teaming (government-industry partnerships) to address remaining technical barriers; and, obtain input from industry (future R&D suggestions, comments on government programs).

For a complete brochure, fill out the form below and mail to: AWS Conferences, 550 N.W. LeJeune Road, Miami, FL 33126, or call 800-443-9353, x 278.

Please send me information on the conference, *"Commercialization of Advanced Joining Technology Through Industry-Government Partnering"*

Name_____

Company_____

Address_____

City_____ State_____ Zip_____

Telephone_____ Fax_____